American Journal of Physics

PAPERS | AUGUST 01 2024

Splitting the second: Designing a physics course with an emphasis on timescales of ultrafast phenomena VIDEO FREE

Igor P. Ivanov

Am. J. Phys. 92, 616–624 (2024)
https://doi.org/10.1119/5.0133767

Splitting the second: Designing a physics course with an emphasis on timescales of ultrafast phenomena

Igor P. Ivanov[a)]
School of Physics and Astronomy, Sun Yat-sen University, 519082 Zhuhai, China

(Received 6 November 2022; accepted 8 May 2024)

Timescales spanning 24 orders of magnitude smaller than one second can be studied experimentally, and each range is packed with different physical phenomena. This rich range of timescales offers a great context for an innovative undergraduate physics course which introduces modern physics and technology from an unconventional perspective. Based on the author's experience in lecturing on these topics to different audiences, this paper proposes a syllabus of a semester-long timescale-based undergraduate physics course.
https://doi.org/10.1119/5.0133767

I. INTRODUCTION

The range of timescales on which physical phenomena unfold is truly staggering. The experimentally accessible range of sub-second timescales covers dozens of orders of magnitude, down to about 10^{-27} s. Every interval on this logarithmic scale is packed with ultrafast phenomena of very different nature. Here, I advocate using this logarithmic timescale as a rich source of context upon which an innovative, customizable lecture course can be built. This course will introduce undergraduate science students to the fascinating world of modern physics from an unconventional perspective.

The idea to categorize physics phenomena according to their duration is not new. In the academic literature, review papers on specific topics often begin with an overview of the spatial and temporal scales involved. Some popular science books (Ref. 1 is a great example) and web pages[2] list timescales of a large variety of phenomena. However, these resources often contain just compilations of numbers and curious facts, mostly unrelated to each other. Little effort is put into creating a coherent educational story line, which would help understand the origins of and the interplay between timescales in different phenomena.

A timescale-based course on ultrafast[3] phenomena can overcome these shortcomings if the lecture material is chosen and organized according to several guidelines. First, it is a good idea to systematically cover various time intervals starting from milliseconds and microseconds down to the shortest measurable intervals. Within each interval, one often finds new "protagonists"—macroscopic bodies, matter, radio waves, molecules, electrons, light, and subatomic particles—as well as characteristic analysis techniques. Second, the course should emphasize timescale-driven connections between areas of physics and provide concrete examples of their interplay. A few examples of these connections are given in Sec. II. Third, it is instructive to explicitly demonstrate how the duration of various phenomena can be estimated through simple order-of-magnitude calculations and to discuss limitations of these estimates. Equipped with these examples, students can be encouraged to make numerical estimates by themselves, which will eventually help them to develop their own "timescale intuition."

The author has the experience of lecturing on these topics at different levels, from a single two-hour lecture for the general public[4] to a series of colloquia for physics researchers.[5] In spring 2023, the author taught this course at the School of Physics and Astronomy, Sun Yat-sen University (China) as an elective undergraduate course open to all students majoring in science. The slides of one of these lectures can be found in the online supplementary material.

The main goal of this paper is to inspire instructors to come up with their own unique timescale-based introduction to modern physics. At the end of this paper, a possible syllabus for a semester-long course of 36 academic hours is outlined, but the reader should not expect to find here a self-contained description of all the topics which could potentially be covered in this course. The main part of the paper will, instead, present a small selection of illustrative situations which exhibit timescales interplay. Hopefully, through these examples, the reader will appreciate the variety of timescale connections that could be shared with undergraduate students and that could serve as an unconventional introduction to many branches of modern physics.

II. EXAMPLES OF TIMESCALE INTERPLAY

A. Converting time into space: From oscillating droplets to high-speed cameras

Although the millisecond range is accessible to human experience, effects lasting only a few milliseconds are usually too fast to be noticed by the unaided eye. However, they can be easily revealed with commercially available cameras and smartphones. In fact, some top-level smartphones are equipped with image sensors stacked with a fast DRAM memory, which enable the user to record short video clips at 960 fps. Such a smartphone, by itself, is a great tool for many in-class and at-home experiments.

How a water jet breaks up into droplets and how these water droplets oscillate are nice millisecond-range phenomena that can be studied with cameras, at home, or in class. These processes are driven by capillary effects, that is, the tendency of the liquid in free fall to minimize its surface area while keeping its volume unchanged. A cylindrical water column with a constant radius is unstable against certain periodic deformations of its radius because such deformations reduce the air–liquid interface area per unit length. Upon multiple pinch-offs, droplets of deformed shapes emerge and are driven by capillary forces toward the optimal

shape, the sphere. As the liquid possesses inertia, droplet deformation does not stop at once when the spherical shape is attained. As a result, the droplet oscillates between oblate and prolate shapes until the oscillations eventually die out due to viscous damping.

Although the exact mathematical description of the above processes may be extremely complicated, their characteristic timescales can be estimated using dimensional analysis, which is a useful skill for students to learn. Given the surface tension coefficient σ of dimension $[\sigma] = \mathrm{N/m} = \mathrm{kg/s^2}$ and the liquid density of dimension $[\rho] = \mathrm{kg/m^3}$, one can construct, for a water droplet of radius r, the unique combination of the correct dimension: the "capillary time" $\tau_c = \sqrt{\rho r^3/\sigma}$. For water, the result is $\tau_c = 4$ ms for $r = 1$ mm and 4 μs for a 10 μm droplet.

The capillary timescale can be used to estimate not only the droplet oscillation period but also other capillary effects with rich dynamics, such as a liquid bubble burst,[6] the instability and breakup of a cylindrical water jet with its nontrivial pinch-off, and the emergence of satellite droplets.[7–9] It may be instructive to mention that a thorough understanding of the microsecond dynamics of micrometer-sized jets and droplets is not of pure academic interest only but is also critical for clean, well-controlled ink-jet printing.[10]

An oscillating liquid droplet possesses another characteristic timescale, which can also be estimated via dimensional analysis: the viscous damping time $\tau_{visc} = \rho r^2/\eta$, where η is the dynamic viscosity coefficient. Viscous damping leads to an exponential decay of the oscillation amplitude, and if $\tau_{visc} \gg \tau_c$, which holds for millimeter- and micrometer-sized water droplets, many oscillations take place before the oscillatory behavior dies out. By equating the two timescales, τ_{visc} and τ_c, one can determine the critical size of the droplet below which liquid motion is overdamped and no oscillations can occur.

How can we measure the millisecond-scale droplet oscillating period? It can be imaged directly using a high-speed camera with thousands of frames per second (fps).[7–9] In fact, one can find on YouTube many impressive videos of various everyday phenomena filmed by slow-motion enthusiasts.[11,12] This can also be done for large water droplets with a smartphone. However, one does not actually need to resort to the costly high-speed video recording equipment in order to measure the droplet oscillation period. This can be done with a single photo taken by a modest, commercially available camera.

The idea is that, when illuminated by a steady collimated light source, a vibrating droplet reflects light in a time-dependent way. Consider a light ray entering the droplet at an impact parameter b from its center, experiencing total internal reflection, and leaving the droplet at an angle θ that depends on b. The dependence of $\theta(b)$ has an extremum θ_r, the angle at which we observe the brightest reflection. Since this optical phenomenon is responsible for the formation of rainbows, the angle θ_r is called the rainbow angle. As the droplet's shape changes periodically, the optical path in a deformed droplet differs from that in a spherical one, which makes the rainbow angle $\theta_r(t)$ oscillate in time. A stationary camera observing the vibrating droplet from an angle close to the rainbow angle sees a strong periodic modulation of the reflected light intensity. This phenomenon has been known for more than a century and recently put to work in time-resolved rainbow refractometry,[13] which allows the investigation of droplet oscillations without imaging its shape.

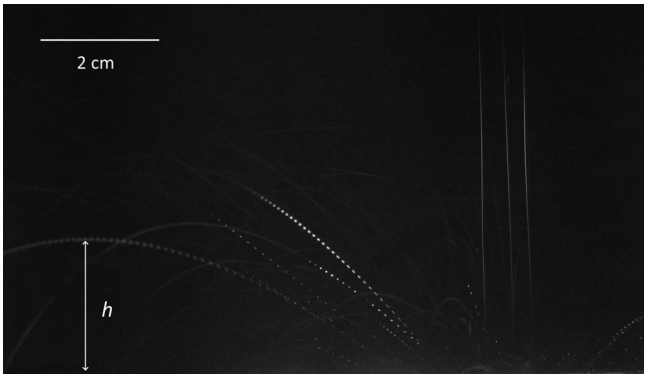

Fig. 1. Measuring the water droplet oscillation period with a long-exposure photo. The label h denotes the apex height of the visible part of the parabolic trajectory.

Put simply, the vibrating droplet becomes a point-like, rapidly flickering source of light. If the droplet moves against a dark background, it leaves a bright dashed trajectory on a long-exposure photograph. By counting the number of dashes, N, within a reference time interval, τ, one can compute the oscillation period $T = \tau/N$. If the entire trajectory of the droplet is fully visible in the image, then τ is just the exposure time. However, one can also rely on a different reference time defined by the free fall dynamics of the droplet itself. Figure 1 shows the light traces left by water droplets falling vertically on a hard surface (a saucer) and breaking upon impact into smaller droplets, which fly away and, naturally, vibrate. The picture was taken with a Canon EOS 100D camera, and, with the exposure time set to 2 s, it captured several impact instances. The dashed trajectories clearly show vibrations of the breakup droplets, while the solid vertical lines, which are produced by the reflections from the large falling droplets, confirm that the illuminating light source was steady. In this specific picture, one can see a parabolic trajectory whose apex height $h \approx 3$ cm could be determined from the experiment geometry. The reference time τ can be calculated as the rise time: $\tau = \sqrt{2h/g} \approx 80$ ms. Although the air drag force affects the droplet motion, its influence is not dramatic, which the reader can verify by observing that the trajectory does not differ too much from the symmetric parabolic curve. Extrapolating the trajectory to the lower edge of the image frame and counting the bright dashes, one estimates that about 40 oscillations took place over the reference time, which yields the oscillation period $T \approx 2$ ms.

This experiment can be the starting point to introduce a family of imaging techniques in which one effectively converts rapid temporal variations of light into a spatially modulated pattern. If the compact light source is stationary, one can take a picture through a rotating mirror, or one can simply rotate the camera itself in the horizontal plane when pushing the trigger button. With this technique, one can "discover" that many LED indicators found at home are in fact blinking with frequencies up to 1 kHz and beyond. It is even more impressive that, thanks to the persistence of human vision, one can train the naked eye to observe a similar sequence of images by swiftly moving one's gaze across a rapidly flickering light source. This phenomenon known as the "phantom array effect" is detectable at flicker frequencies up to several kilohertz.[14] The author confirms observing it at least up to 1.5 kHz.

In the 19th century, the rotating or vibrating mirror technique played a role in studies of fast processes. In 1855, Jules Antoine Lissajous, looking at a small light source through a pair of perpendicularly vibrating mirrors, observed what we now call the Lissajous figures.[15] In 1870s, Rudolph König used the manometric flame apparatus he had invented to visualize, for the first time, the acoustic waveforms produced when pronouncing various vowels. Together with his assistant, he was observing the rapidly oscillating flame with the aid of a rotating mirror and sketched the patterns in his laboratory notebook.[16] In the late 1850s, Berend Wilhelm Feddersen used a fast rotating mirror to measure the duration of the spark discharge of a Leyden jar and discovered that this ultrafast process had a non-trivial temporal structure which included several damped oscillations of the electric current across the spark gap.[17]

The rotating mirror is also a central part of a family of ultrahigh-speed cameras capable of taking millions of frames per second (Mfps). The high-speed cameras of the early 20th century[18] reached thousands of fps, but going beyond tens of kfps put too much mechanical stress on the film and its drive mechanism. One of the ideas was to keep the film stationary by attaching it to the inner surface of a large hollow drum, and to place a fast rotating mirror in the focal plane of the camera, see Fig. 2. The evolving scene of an ultrafast process was sliced by a shutter into a rapid succession of images, which are reflected by the rotating mirror as successive frames on the film, allowing one to shoot short sequences at Mfps frame rates. These cameras were initially developed during World War II to support the development of the atomic bomb,[19] but their capabilities were further expanded in the post-war years.[20–22] For instance, the CP5 camera had a mirror rotating at $f = 5500$ revolutions per second, which translates into the angular velocity $\omega = 2\pi f \approx 35\,000\ \mathrm{s}^{-1}$. The angular velocity of the reflected image is twice as large, and, for the drum radius $R = 1$ m, one gets the linear velocity of the image across the film: $v = 4\pi f R = 70$ km/s. With a 8 mm frame height plus some interframe distance, one ends up with 8 Mfps, which was indeed the frame rate achieved by CP5, see Chap. 25.11 of Ref. 21. An obvious drawback of the fixed-drum rotating mirror camera is that one can only record a limited number of frames; CP5 had the capacity of 117 frames in one go. Modern ultrahigh-speed cameras, such as Brandaris 128 taking up to 768 images at 25 Mfps,[23] acquire images with sensor arrays rather than films, but they still rely on the rotating mirror technique.

The same idea—measuring very short time intervals by converting time into space—is used in slit photography and in the photo finish systems[20,21] and can also go beyond visible light. The classic oscilloscope, one of the main tools of 20th century electrical engineering, exploits the same principle down to the nanosecond range: a generator sweeps the electron beam horizontally across the cathode ray tube (CRT) screen, and the waveform of a rapidly varying voltage, applied vertically, is seen on the screen. Electro-optical systems, operating either in the intermittent or streak mode, make use of the electron beam manipulation for detecting rapid variations of light intensity. The incoming light hits the photocathode producing a variable electron flux. The electrons are accelerated toward the CRT screen, but, being swept inside the tube, leave a spatially modulated image on the screen. Coupled with a spectrograph, the electro-optical streak camera is often used in molecular physics to obtain time-resolved spectra of rapidly evolving fluorescent light emitted by organic molecules.[24]

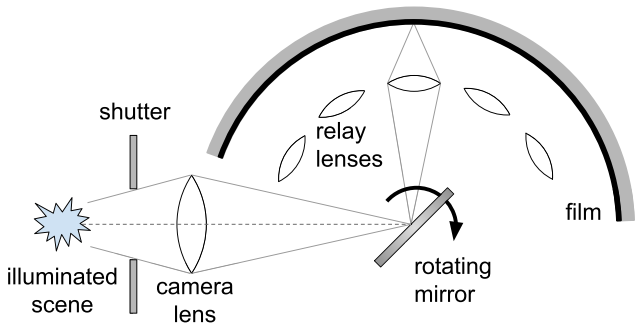

Fig. 2. Principle of the rotating mirror ultrahigh-speed camera.

B. Ultrasound and its limits

The shorter the timescales, the smaller are the length scales involved. This link between the two scales becomes particularly evident when discussing waves with an approximately linear dispersion relation, such as electromagnetic waves or ultrasound.

Discussing ultrasound in an undergraduate science-major class can start with the acoustic frequency scale drawn together with the wavelength scale, with air or water as the reference medium. After marking the audible frequency range, the instructor can ask the students whether the frequency scale has natural limits or extends infinitely in both directions. Many students readily point out that discreteness of matter places a lower bound of the ultrasound wavelength $\lambda > 2a$, where a is a typical intermolecular distance. Using the typical sound velocity in liquids and solids, $c_s \approx$ a few km/s, one can estimate the upper end of the ultrasound frequency scale as $f = c_s/\lambda \sim 10$ THz.

Placing the lower limit on the ultrasound wavelength in air may be less intuitive for the students. Guided by the instructor, the students should arrive at the conclusion that the relevant length scale is not the intermolecular distance but the much longer mean free path in air. During this discussion, one may need to recapitulate the concept of mean free path and emphasize its dependence on the scattering cross section. Using the known density of air under normal conditions, the students can estimate the mean free path ($\ell \approx 65$ nm) and find that the ultrasound frequency scale in air ends at about 1 GHz. Since this value depends on the air density, one can repeat the same estimate for gases under conditions very different from normal, such as the extremely rarefied interplanetary medium. Another thought-provoking question is what happens if a plate vibrating at a multi-GHz frequency is exposed to air. Will it emit sound, and if not, what exactly will happen? Such discussions will help students develop their molecular dynamics intuition.

Practical applications of ultrasound offer a rich context for discussing the interrelations between lengths, timescales, and frequency ranges. The relevant literature is vast; numerous examples can be found in historical essays,[25,26] textbooks,[27] and encyclopedic resources such as Chap. 21 of Ref. 28. When presenting examples of ultrasound imaging, one should stress that the ultrasound frequency choice is often directly determined by the geometrical scale of the objects of interest, from bats hunting for millimeter-sized insects to sonography (medical ultrasound imaging) of various organs.

Another key parameter, which acts as a limiting factor in many applications, is the frequency-dependent sound attenuation in fluids. For example, when selecting the operating frequency in sonography, one seeks a balance between two requirements: the frequency must be sufficiently high to achieve high resolution but, at the same time, should be low enough in order to avoid attenuation beyond the detectability limit of the ultrasonic signal reflected from the desired depth inside the patient's body.

Here, is an example which provides some intuition on the timescales involved in sonography. Prenatal ultrasound, a standard procedure during pregnancy, enables observation of a moving fetus in real time. What makes this real-time video possible is the interplay of several timescales. The typical operating frequency $f = 4$ MHz corresponds to an oscillation period of 0.25 μs. A short ultrasonic pulse of duration $\tau = 1$ μs is sent into the body by the transducer and results in the depth resolution of about $c_s\tau \sim 1$ mm. At 4 MHz, the attenuated ultrasound echo can be detected from the depth up to about $d = 15$ cm. Once a short ultrasonic pulse is emitted, we need to wait $\Delta t = 2d/c_s = 200$ μs before sending a new pulse. During this "silence period," we record the echo returning from all the depths up to d. Thus, we can obtain a one-dimensional density profile along the direction of the ultrasonic beam $1/\Delta t = 5000$ times per second. The transducer does not, of course, send the ultrasonic pulse along the same direction all the time but rather "rocks the beam," that is, sweeps the directions within a certain planar angle within a specific plane. Assuming that 100 one-dimensional scans along different directions are enough to construct a two-dimensional image,—which is close to what modern ultrasound scanners do, see Chap. 21.4.3 of Ref. 28,—we conclude that the full two-dimensional view can be updated $5000/100 = 50$ times per second. This is enough for a smooth, real-time video recording.

There is also a lot of interesting physics at the high end of the frequency scale. 1 THz corresponds to an oscillation period of 1 ps and to wavelengths of a few nanometers at most. We approach the timescales of thermal atomic or molecular motion in condensed matter and the distances at which discreteness of matter becomes important. As a consequence, we can expect the properties of ultrasound to change in the THz frequency range compared with the low-frequency limit.

To illustrate this point, let us mention the curious story of the so-called "fast sound" in water. In one of the first molecular dynamics (MD) simulations[29] of a system of 216 water molecules performed back in 1974, two types of oscillation modes were observed, corresponding to two different sounds in water, with the high-frequency sound propagating at $c_s \sim 3$ km/s. The small size of the simulated system corresponded to wavelengths of 1–2 nm, beyond the reach of the experimental methods available at the time. A decade later, though, the high-frequency sound was confirmed experimentally,[30] but its origin and properties were still debated.[31] One explanation was that, at the picosecond scale, the ephemeral network of hydrogen bonds acquires extra rigidity, which increases the speed of the usual longitudinal mode (making it the "fast sound"). At the same time, the picosecond-scale rigidity of the hydrogen bond network helps water elastically—or better to say, viscoelastically—resist to very fast shear displacements. Instead of the steady shear flow controlled by viscosity, which is observed in water at constant or slowly changing shear stress, at ultrahigh frequencies, water supports propagating transverse vibrations, the "transverse sound." In an alternative explanation, water was viewed as a mixture of two interacting fluids of heavy and light atoms, and the fast sound was associated with certain features of the frequency vs wavenumber curve which are typical for such mixtures.

Both explanations agreed with the data at the high and at the low ends of the frequency scale, but differed at intermediate frequencies. To settle the issue, it was necessary to experimentally observe how the structural modifications of sound propagation set off in the GHz range, which proved to be experimentally challenging. Indeed, megahertz frequencies are well covered by traditional ultrasonic experiments, while the oscillation dynamics in the THz range is studied in a completely different way, via inelastic scattering of neutrons or x rays. As a result, there existed a vast frequency gap between the two domains exhibiting such different ultrasound properties. Only in 2006, with the advent of new scattering experimental data covering a significant part of the GHz range, was this gradual change in the speed of sound directly measured, in a clear support of the viscoelastic model.[32]

C. Positrons in matter

Within the nanosecond range, there is a beautiful example of a technology which stems from the interplay between the timescales of two very different effects. The phenomenon in question is the behavior of positrons inside solid matter before they eventually annihilate, and the technology bears the name of the positron annihilation lifetime spectroscopy (PALS).[33,34]

A lecture on this topic can begin with a general discussion of antiparticles and antimatter. Many students, even before taking a formal particle physics course, are familiar with the concept of antimatter as it appears in many science fiction movies. However their acquaintance may reveal certain misconceptions, such as the popular but erroneous statement that "antiparticles travel back in time." After a general introduction on the topic which can straighten out the possible misconceptions, the discussion can move on to the main question: what happens when a positron enters a dense medium? Most students know about annihilation, but they most likely have never asked themselves how quick this process is. They may picture it as something instantaneous: the positron travels from vacuum into the sample and, upon encountering the first atom, annihilates with one of its electrons.

Posed in the timescale-based course, this question by itself may lead the students to suspect that the positron could in fact travel a certain distance inside the medium before annihilating. For the quantitative discussion, it is instructive to rephrase this question in terms of mean free path and cross section, which are concepts students should be familiar with from the kinetic theory of gases. In gases, the molecules can only scatter, not annihilate, and one calculates the mean free path from their scattering cross section. The positron moving through a dense medium also scatters from the electrons, $e^+e^- \to e^+e^-$, with the scattering cross section σ_s. The direct annihilation $e^+e^- \to \gamma\gamma$ represents an additional, competing process, characterized by its own annihilation cross section σ_a. Thus, for an electron density n, one can introduce the mean scattering length $\ell_s = 1/(n\sigma_s)$ as well as the mean annihilation length $\ell_a = 1/(n\sigma_a)$, the typical distance the

positron travels before annihilation. What happens first, scattering or annihilation, depends on the ratio of the two cross sections.

Quantum electrodynamics allows one to accurately calculate the annihilation cross section.[35] For a non-relativistic positron moving with the dimensionless velocity $\beta = v/c \ll 1$, one gets $\sigma_a = \pi\alpha_{em}^2\lambda_C^2/\beta$, where $\alpha_{em} \approx 1/137$ is the fine structure constant and $\lambda_C \approx 0.4$ pm is the reduced Compton wavelength of the electron. If we assume that the positron is thermalized, its thermal velocity being $\beta = 4 \times 10^{-4}$, $v = 120$ km/s, we can estimate the annihilation cross section: $\sigma_a = 6 \times 10^{-22}$ cm^2. Using the typical electron density in crystals, one obtains the annihilation length $\ell_a \sim 100$ μm, which is nearly a million times the typical interatomic distance. For a more energetic positron with the kinetic energy in the kiloelectron-volt range, which is a typical value for impinging positrons in their materials science applications, the cross section further drops by at least two orders of magnitude ($\sigma_a = 3 \times 10^{-24}$ cm^2 for $E_{e^+} = 1$ keV), and the annihilation length increases proportionally. We arrive at the following conclusion which may surprise the students: the distance the positron travels in matter before annihilation is truly huge compared to atomic scales, and the corresponding time is of the order of a nanosecond.

The cross section of the positron scattering in matter can also be computed with quantum electrodynamics. Scattering of a sufficiently energetic positron from atoms is usually accompanied by atom excitation or ionization and leads to energy loss for the positron. Details of the cross section calculation depend in a significant way on the energy and on the atom itself. To get the simplest order-of-magnitude estimate, we can disregard the bonding energy of the atomic electrons and view the collision as an elastic e^+e^- scattering. Furthermore, if we focus on the scattering events in which the positron direction changes by a large angle, we can estimate the cross section as $\sigma_s \sim \alpha_{em}^2\lambda_C^2/\beta^4$, which, for non-relativistic positrons, is much larger than σ_a. Alternatively, one can rely on experimental data for the positron scattering from atoms,[36] which show the scattering cross section in the ballpark of $\sigma_s \sim 10^{-20}$ cm^2 for $E_{e^+} = 1$ keV, much larger than σ_a. Thus, the positron entering a dense medium will most likely experience multiple collisions, lose energy, and, perhaps, thermalize within a timescale much shorter than a nanosecond and well before annihilating.

In addition to scattering and direct annihilation, the slow positron can capture an electron to form an e^+e^- bound state, the positronium. It is known that positronium can come in two versions: the parapositronium (p-Ps) with spin zero, which lives τ(p-Ps) = 0.125 ns and annihilates into two photons, and the orthopositronium (o-Ps) with spin one, which must produce at least three photons upon annihilation and, therefore, lives much longer, τ(o-Ps) = 142 ns. The gap by three orders of magnitude between the two lifetimes comes from one more power of α_{em} required to create the extra photon in the o-Ps annihilation and a numerical coefficient related to the phase space of the final photons (it is, of course, up to the instructor to determine how much of this information is explained to the students).

Now comes the crucial point which enables one to measure the average pore size in a nanoporous material.[33,34] The value τ(o-Ps) = 142 ns refers to the decay of orthopositronium in vacuum. However, inside matter, due to the constant interaction with atoms and electrons, the lifetime can be dramatically reduced to a fraction of nanosecond. However, the reduction is less severe if the medium is porous: the o-Ps has a chance to exit the dense matter into a pore and stick around for some time. Measurements show that τ(o-Ps) as a function of the pore size d begins to depart from its vacuum value for pores smaller than 100 nm, goes below 100 ns around $d = 10$ nm, and further below 10 ns for $d \sim 1$ nm. Thus, the o-Ps lifetime determination is a convenient method to measure porosity and the typical pore size of nanoporous materials. What one needs is to irradiate the sample with an intense short positron pulse, disregard the prompt photon peak coming from parapositronium or direct e^+e^- annihilation within the first nanoseconds, and focus on the late time (up to 1 μs) exponential tail of the delayed photons. In this way, one gets a nanometer-scale diagnostic tool through a macroscopic counting technique.

In a highly porous material, the pores can form a network, which the o-Ps particles can efficiently explore during their lifetime. Taking a pore size of several nanometers and estimating the diffusion path length to tens of microns, one sees that a single o-Ps can explore at least hundreds of pores before annihilation. If sufficiently many positrons are implanted in the sample, some of them can meet inside a pore to form molecular positronium Ps_2; an experimental evidence of its formation was reported[37] in 2007. Let us stress again that all these remarkable phenomena are possible due to the significant gap between the o-Ps lifetime and the time between its successive scattering events with the surface atoms of the medium as it travels across the pore network.

D. The puzzle of ultrafast melting

When we discussed in Sec. II A the vibration of a water droplet and, in Sec. II B, the propagation of ultrasonic waves in solids, we were dealing with smooth motion of continuous matter. This was possible because the timescales involved were much longer than picoseconds, so that many molecules or atoms in a liquid or a solid were simultaneously affected by the phenomenon. However, around 0.1–1 ps, collective motion breaks down into "elementary steps," that is, jerks and collisions of individual molecules. This molecular agitation effectively freezes as we go deep into the femtosecond range. It is, therefore, natural to expect that the fastest structural changes in condensed matter, such as ultrafast melting of crystals, must take at least a few picoseconds.

In a typical experiment on ultrafast melting, one sends an intense, ultrashort focused laser pulse with duration $\ll 1$ ps onto a crystal sample. The pulse is absorbed by a thin surface layer, transmitting its energy to the electrons, which quickly, within 100 fs, form a very hot electron gas. However, the ions remain cold during this sub-picosecond absorption stage. Indeed, they could heat up via collisions with hot electrons, but the electron-to-ion energy transfer is not instantaneous. With the typical velocity of $v \sim 1000$ km/s, the free electrons collide with ions on the femtosecond timescale. This seems fast. However, in a single collision, the electron transmits only up to $2m_e/M_{ion} \sim 10^{-4}$ of its energy to the ion (recall the classical mechanics problem of a small mass elastically colliding with a massive body at rest). Thus, one needs a few thousand electron–ion collisions to significantly heat up the ion lattice. This is why it takes at least a picosecond for the ultrashort laser pulse to locally melt the crystal.

The above estimate is, by itself, an instructive exercise as it illustrates the significant timescale gap between the

dynamics of light, swift electrons, and heavy, sluggish ions. However, it is also the entry point to a puzzle which took a couple of decades to solve. Namely, starting from 1983, experimental evidence[38] kept accumulating that, at very high pulse intensities, local melting occurs within a fraction of picoseconds, significantly faster than the above estimate. After intense studies, it was finally demonstrated[39,40] that this surprisingly fast melting is of non-thermal nature. When the laser pulse removes the majority of the valence electrons from the ions, the chemical bonding which keeps the crystal structure rigid becomes much weaker, and the ions readily fly away from their initial positions. The key point is that it happens even before the ions heat up. Since the typical periods of the thermal vibration of atoms or ions in a crystal at room temperature are in the hundreds fs range, one can expect that the crystalline order can be effectively destroyed within half a period or so. In a real situation, the thermal and non-thermal mechanisms compete, but modern molecular dynamics simulations, which take into account the hot free electrons, confirm that structural disorder sets in within half a picosecond after the absorption of an intense ultrashort laser pulse.[40]

E. Measuring the lifetimes of unstable particles

Metastable atomic nuclei and elementary particles have lifetimes that span dozens of orders of magnitude,[1] from the lifetime of the Z-boson[41] ($\tau_Z \approx 2.6 \times 10^{-25}$ s), the mediator of the neutral weak interaction, to the half-lives of extremely long-lived nuclides that exceed the age of the Universe. Not going into the fundamental origin of lifetimes being so different, we only mention here various methods to measure short-lived particles and nuclei.

The muon μ, the heavy metastable analog of the electron, unexpectedly discovered in 1937 while studying cosmic rays,[42] lives about $\tau_0(\mu) = 2\,\mu$s and decays to an electron and a pair of neutrinos. Its lifetime is huge by subatomic standards; even a non-relativistic muon can travel a macroscopic distance, which can be measured directly. Discussing the muon lifetime is a perfect place to introduce relativistic time dilation. The above value τ_0 refers to the muon's lifetime at rest. If it moves with velocity v, its decay, as observed in the laboratory reference frame, slows down, and we see it live longer: $\tau = \gamma\tau_0$, where $\gamma = (1 - v^2/c^2)^{-1/2} = E/(mc^2)$ is the Lorentz factor. In fact, without time dilation, we would not be able to detect the cosmic ray muons using ground observations. Indeed, they are produced high in the atmosphere, at the height of about $h = 15$ km. Dividing this height by the speed of light gives 50 μs, which is 25 times larger than τ_0. However, if the initial muon energy is larger than 5 GeV, its initial γ-factor exceeds 50. Although such muons lose a part of their energy on their way to the ground, most of them reach the sea level. Numerous practical applications of muons, such as muon tomography and radiography of cargo vehicles, large structures, and even active volcanoes,[43] would be impossible without time dilation.

The lifetimes of the so-called strange hadrons, which began appearing in accelerator experiments in the late 1940s,[1,42] cluster around 0.1–1 ns, with the exception of kaons, which live tens of nanoseconds. However, a nanosecond multiplied by the speed of light gives the macroscopic distance of 30 cm, which grows further when time dilation is accounted for. Thus, exploration of strange hadrons poses no problem: one can directly observe the ionization tracks left by the charged strange hadrons in a sensitive medium.[42]

The collider experiments of the 1970s and 1980s brought to light two new families of particles: the charmed and beauty hadrons.[35] These hadrons contain a heavy quark, c or b, which decays via weak interactions. Interestingly, these two families have lifetimes that fill a rather narrow interval: from about 0.1 to 2 ps.[1,41] Three orders of magnitude shorter than the strange hadron decays, these lifetimes can still be measured directly by detecting the distance these particles travel between the production and decay points.

To illustrate how this is done in modern collider experiments, imagine a high-energy collision taking place inside a vacuum pipe with a diameter of a few centimeters. Tens of charged particles can be produced in this collision. If long-lived, they exit the beam pipe and pass through the sensitive elements of a multi-layered cylindrical detector. The tracks they leave across the detector seem to emerge from a single primary vertex, the spot where the collision took place, see Fig. 3, top.

Detecting a short-lived hadron containing a heavy quark (let it be the D-meson, for definiteness) and measuring its lifetime in such a busy environment are not easy tasks. One picosecond multiplied by the speed of light gives the distance $d = 0.3$ mm. Both the production point (the primary vertex) and the decay point (the secondary vertex) of the D-meson are located inside the vacuum pipe. As a result, the detector sees not the D-meson itself but only its decay products.

Fortunately, the very central part of the detector, called the vertex detector, can accurately reconstruct the passage of individual particles through each of its cylindrical layers, see Fig. 3, bottom. Extrapolating each trajectory, we can find the point inside the beam pipe where it crosses with the trajectories of many other particles. In this way, we can distinguish

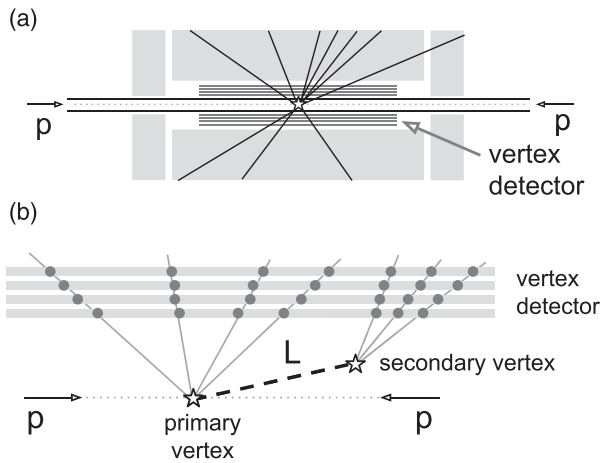

Fig. 3. Top: schematic side view of a cylindrical particle detector at a proton collider. Charged particles produced in proton (p) collisions leave tracks across the detector, which are measured with a high accuracy in the vertex detector. Bottom: zoomed view on the central part of the detector, showing the first few layers of the vertex detector. A high-energy proton collision takes place at the primary vertex and leads to the production of many hadrons, which can include a short-lived hadron (heavy dashed track). The short-lived hadron travels distance d inside the beam pipe and decays into daughter hadrons at another point (the secondary vertex). By measuring and extrapolating the trajectories of all the charged particles, the vertex detector accurately locates the primary and secondary vertices and measures their sub-millimeter distance.

hadrons emitted from the primary vertex and a group of particles emerging from the secondary vertex lying at a distance. The location of the two points can be determined with an accuracy of tens of micrometers, which is enough to measure picosecond-scale lifetimes.

Actually, the displacement of an unstable particle can be detected even if it does not exceed the atomic scale. This method is called the crystal blocking technique and is used in nuclear physics to detect unstable nuclei with half-lives of the order of attosecond ($1\,\text{as} = 10^{-18}\,\text{s}$). Consider a projectile nucleus traveling at speed $\sim 0.2\,c$ and colliding with a target nucleus in a crystal to produce a short-lived heavy isotope, Fig. 4. Due to momentum conservation, this heavy short-lived nucleus keeps moving, its velocity being of the order of $\sim 0.1\,c$. However, if the compound nucleus half-life is much shorter than 1 as, it shifts from its original position by a distance much smaller than $1\,\text{as} \times 0.1\,c = 0.3\,\text{Å}$, and its fission occurs within the same crystallographic plane. The fission products are stable, can be emitted at different angles and leave the sample approximately keeping its initial direction. However, those fission fragments which are initially emitted along the plane will be deflected away by the repulsive Coulomb force of the ions sitting within the same crystallographic plane. Therefore, a detector measuring the angular distribution of the fission fragments will observe depletion (the "shadow") of fragments in the direction parallel to the crystallographic plane, Fig. 4, left. However, if the nucleus survives for at least 1 as, it has time to move into the space between the planes, Fig. 4, right. The fission products emitted along the crystallographic plane will not be significantly deflected, since their trajectory is sufficiently far away from the other nuclei in the same plane. The detector will now see fission fragments emitted in all directions, including parallel to the plane, and the shadow gets weaker or even disappears altogether. This method was used[44] to detect the attosecond-scale lifetime of certain isotopes of elements 120 and 124.

Shorter lifetimes, belonging to the zeptosecond ($1\,\text{zs} = 10^{-21}\,\text{s}$) and yoctosecond ($1\,\text{ys} = 10^{-24}\,\text{s}$) time ranges, are measured indirectly, via the energy–time uncertainty relation.[45] Applied to an unstable particle, it links its lifetime τ with the width Γ of its resonance curve on the plot of the relevant cross section as a function of the collision energy: $\tau = \hbar/\Gamma$, where $\hbar$ is the reduced Planck's constant which can be conveniently expressed as $\hbar \approx 0.66\,\text{fs}\cdot\text{eV} = 0.66\,\text{zs}\cdot\text{MeV}$. For example, in a very recent study,[46] the tetraneutron ^{4}n—a quasibound state of four neutrons without any proton—was unambiguously observed in the transfer reaction $\text{p}+^8\text{He} \rightarrow \text{p}+^4\text{He}+^4\text{n}$ as a clear peak when plotting the number of detected events as a function of the energy of the four-neutron system. Its width $\Gamma \approx 1.75$ MeV corresponds, via the uncertainty relation, to the tetraneutron lifetime of 0.4 zs, one of the shortest timescales ever measured in nuclear physics.

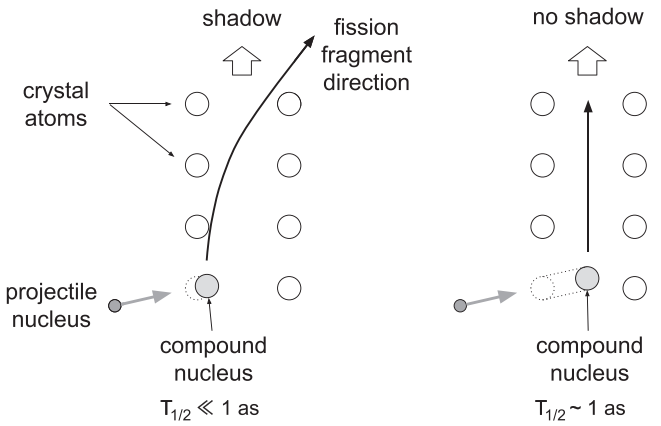

Fig. 4. The principle of the crystal blocking technique to detect the attosecond-scale half-life of an unstable nucleus.

In the world of elementary particles, excited hadrons appear as broad resonances in the hadron scattering cross sections with $\Gamma \sim 100$ MeV, which translates into 7 ys. This is close to the "hadronic time" τ_h, the minimal timescale on which we can talk about hadrons. It can be estimated by dividing the hadron size $\approx$1 fm by the speed of light, which gives $\tau_h \approx 3$ ys. In what concerns particle lifetimes, the record holder is the Z-boson, the heavy mediator of the neutral weak interactions. It is visible as a spectacular resonance peak in the cross section of the e^+e^- annihilation into hadrons, standing nearly a thousand times higher than the non-resonant cross section, see Chap. 53 of Ref. 41. Measured at the LEP collider at CERN with unprecedented precision, it exhibits the width $\Gamma_Z \approx 2.5$ GeV, from which one deduces the extremely short lifetime $\tau = 0.26$ ys (or 260 rontoseconds, if we use the recently approved[47] SI prefix ronto-, 10^{-27}).

III. BUILDING THE SYLLABUS

The examples described above show what kind of timescale-based lessons could be drawn from modern physics and technology. However, bringing them together in a single coherent course requires substantial work from the instructor, both in terms of learning and selecting the material.

Table I outlines a possible syllabus for a semester-long undergraduate course of 36 academic hours. In addition, the online supplementary material contains the slides of one of the author's lectures within the course "The world of ultrafast phenomena" given at the Sun Yat-sen University, China.

The possible syllabus in Table I covers a large variety of areas, spanning from classical physics and the development of measurement technology to quantum topics including nuclear and particle physics. This collection of topics is by no means complete nor obligatory; each instructor can build a unique course according to their own preferences. Since the course is aimed at undergraduate physics and science-major students who may not have had a quantum mechanics course, the advanced physics topics are not meant to be taught systematically. The instructor is supposed to select vivid timescale-related illustrations, which could be presented at that level together with basic numerical estimates, and put them in appropriate context.

About one third of the syllabus proposed in Table I deals with the history of various branches of physics and technology. Experience shows that, with such historical excursions, the audience appreciates the human side of the physical world exploration and gets a better perspective on today's achievements and challenges. Certainly, this material can be shortened or expanded according to the instructor's plan. For example, an 18-h syllabus could skip lengthy historical excursions and reduce the number of illustrative examples, keeping the major areas mentioned in the table and mentioning the main experimental techniques, such as direct imaging, ultrashort laser, pulses and the pump–probe method, and

Table I. A possible syllabus for a 36-h course.

Topic	Timescale ranges	Hours
Everyday phenomena, fracture, droplets and jets, photographic, and smartphone experiments	ms, μs	4 h
High-speed imaging: 19th century photography (exposure time from minutes to microseconds), evolution of ultrahigh-speed cameras, and the current state-of-the-art	ms, μs, ns, ps	2 h
Acoustics and ultrasonics: history, experiments, basic spectral analysis, and ultrasound applications	ms, μs, ns, ps	4 h
Electric oscillations and electromagnetic waves: history (from Leyden jar to electric circuits), cathode ray tube and oscilloscope, discovery of radio waves, and AM/FM modulation	μs, ns, ps	4 h
From matter to atoms: collective motion at the ns timescale (crack propagation, ablation, sonoluminescence), molecular motion and molecular dynamics simulation, protein folding, and extreme ultrasound	ns, ps	4 h
The atom: the atomic size, Bohr's model, timescale estimates, excited atoms, and their lifetimes	Down to as	2 h
The femtosecond world: molecular oscillations, electrons in atoms, femtochemistry, and femtobiology	fs, as	2 h
Short laser pulses: history, key parameters, pump–probe technique, and attosecond science	ns, ps, fs, as	4 h
Nuclear processes: estimates, nuclear processes and their timescales, heavy helium isotopes, uranium isotopes, time–energy uncertainty relation, and experimental techniques	Down to zs	4 h
Elementary particles: estimates, lifetimes and time dilation, experimental techniques, and relativistic nuclei collisions	Down to ys and below	4 h
Students' presentations	...	2 h

spectral analysis in various forms including the energy–time uncertainty relation.

There are other degrees of freedom along which the course could be customized, such as the level of the target audience. When lecturing to physics graduate students and researchers, one can assume a higher level of physics knowledge including some quantum topics.[5] The syllabus could include more practical applications, with further technical details, and interesting connections across physics domains rooted in (mis)matching timescales. In contrast, a series of popular science lectures to high-school students may skip many technical and historical aspects and focus on visual content, on interactive discussions which stimulate imagination, on experimental demonstrations and educational games. However, even at this level, the lectures should actually teach the school students a few basic skills such as making numerical estimates based, at least, on the uniform motion formula.

It is also possible to deliver a single two-hour popular science lecture in which one can introduce the entire range of experimentally accessible timescales and illustrate it with a selection of remarkable phenomena.[4] If needed, such a lecture could also include geophysical and astronomical phenomena of very long duration, see Ref. 1 for possible topics and examples.

In summary, there is immense amount of educational material related to durations of physical processes, which is not yet fully exploited beyond pure academic publications. Timescales much shorter than one second can become a central theme in a unique undergraduate physics course which would introduce modern physics from an unconventional perspective. The length, the selection of material, the depth of treatment, the amount of historical details can be adjusted according to the instructor's preferences. As there is no single textbook which could provide all the necessary material, the motivated instructor should invest significant time and effort into learning a vast range of topics and building his/her own syllabus. However, the outcome will be rewarding. In this paper, I tried to illustrate what kind of non-trivial interplay between timescales of different phenomena could be shown in this course. I hope that these examples and the possible syllabus outlined in Table I will inspire physics teachers and educators to build their own unique timescale-focused lecture courses.

SUPPLEMENTARY MATERIAL

Please click on this link to access the supplementary material, which includes details on Igor Ivanov's "Acoustics and ultrasound" lecture given at the Sun Yat-sen University, China. Print readers can see the supplementary material at https://doi.org/10.60893/figshare.ajp.c.7222461

AUTHOR DECLARATIONS

Conflict of Interest

The author has no conflicts to disclose.

[a]Electronic mail: ivanov@mail.sysu.edu.cn, ORCID: 0000-0001-7068-2930.

[1]G. 't Hooft and S. Vandoren, *Time in Powers of Ten: Natural Phenomena and Their Timescales* (World Scientific, Singapore, 2014).
[2]Wikipedia page, see <https://en.wikipedia.org/wiki/Orders_of_magnitude_(time)> for "Orders of Magnitude (Time)."
[3]I focus here on ultrashort timescales because the world of ultrafast phenomena tends to be richer than of ultraslow processes. The proposed course could also include topics from geophysics and astronomy which involve timescales much longer than one second.
[4]Igor Ivanov, "Splitting the second," popular science lecture (in Russian), <https://www.youtube.com/live/pWSWjaPGPiM?si=A-SYQjRE1_02oy9S>.
[5]Igor Ivanov, "Timescales: Travelling Deep into the Second," a series of educational lectures given at JINR, Dubna (Russia), <https://dlnp-update.jinr.ru/en/education-outreach/lectures/1029>.
[6]James C. Bird, Riëlle de Ruiter, Laurent Courbin, and Howard A. Stone, "Daughter bubble cascades produced by folding of ruptured thin films," Nature **465**(7299), 759–762 (2010).
[7]Jens Eggers and Emmanuel Villermaux, "Physics of liquid jets," Rep. Prog. Phys. **71**(3), 036601 (2008).
[8]Wim van Hoeve, Stephan Gekle, Jacco H. Snoeijer, Michel Versluis, Michael P. Brenner, and Detlef Lohse, "Breakup of diminutive Rayleigh jets," Phys. Fluids **22**(12), 122003 (2010).
[9]Sigurdur T. Thoroddsen, Takeharu Goji Etoh, and Kohsei Takehara, "High-speed imaging of drops and bubbles," Ann. Rev. Fluid Mech. **40**, 257–285 (2008).
[10]Arjan van der Bos, Mark-Jan van der Meulen, Theo Driessen, Marc van den Berg, Hans Reinten, Herman Wijshoff, Michel Versluis, and Detlef Lohse, "Velocity profile inside piezoacoustic inkjet droplets in flight: Comparison between experiment and numerical simulation," Phys. Rev. Appl. **1**(1), 014004 (2014).

[11]Youtube channel, see <https://www.youtube.com/user/theslowmoguys for "The Slow Mo Guys."
[12]Youtube video on channel Smarter Every Day, see <https://youtu.be/ADD7QlQoFFI> for "Secret of Snapping Spaghetti in Slow Motion."
[13]Q. Lv, Y. Wu, C. Li, X. Wu, L. Chen, and K. Cen, "Surface tension and viscosity measurement of oscillating droplet using rainbow refractometry," Opt. Lett. **45**(24), 6687–6690 (2020).
[14]J. E. Roberts and A. J. Wilkins, "Flicker can be perceived during saccades at frequencies in excess of 1 kHz," Light. Res. Technol. **45**(1), 124–132 (2013).
[15]J. Lissajous, "Mémoire sur l'étude optique des mouvements vibratoires," Ann. Chim. Phys. **51**, 147 (1857).
[16]David Pantalony, "Seeing a voice: Rudolph Koenig's instruments for studying vowel sounds," Am. J. Psych. **117**(3), 425–442 (2004).
[17]B. W. Feddersen, "LVIII. Contributions to the knowledge of the electric spark," London, Edinburgh, Dublin Philos. Mag. J. Sci. **16**(110), 503–516 (1858).
[18]Youtube video of Lucien Bull's ballistic experiments (1904) recorded at 1500 fps, <https://youtu.be/RLR-LT55Ueo>.
[19]Webpage "High-Speed Photography" from the Atomic Heritage website, <https://www.atomicheritage.org/history/high-speed-photography>.
[20]Graham Saxby, *The Science of Imaging: An Introduction*, 2nd ed. (CRC Press, Boca Raton, FL, 2010).
[21]Sidney Ray, *Scientific Photography and Applied Imaging* (Focal Press, Waltham, MA, 1999).
[22]P. W. W. Fuller, "An introduction to high speed photography and photonics," Imaging Sci. J. **57**(6), 293–302 (2009).
[23]Chien Ting Chin, Charles Lancée, Jerome Borsboom, Frits Mastik, Martijn E. Frijlink, Nico de Jong, Michel Versluis, and Detlef Lohse, "Brandaris 128: A digital 25 million frames per second camera with 128 highly sensitive frames," Rev. Sci. Instrum. **74**(12), 5026–5034 (2003).
[24]Aleksander A. Kubicki, Piotr Bojarski, Marek Grinberg, Michał Sadownik, and Benedykt Kukliński, "Time-resolved streak camera system with solid state laser and optical parametric generator in different spectroscopic applications," Opt. Commun **263**(2), 275–280 (2006).
[25]Katherine A. Kaproth-Joslin, Refky Nicola, and Vikram S. Dogra, "The history of US: From bats and boats to the bedside and beyond," Radiographics **35**(3), 960–970 (2015).
[26]William D. O'Brien, Jr. and Floyd Dunn, "An early history of high-intensity focused ultrasound," Phys. Today **68**(10), 40–45 (2015).
[27]Dale Ensminger and Leonard J. Bond, *Ultrasonics: Fundamentals, Technologies, and Applications*, 3rd ed. (CRC Press, Boca Raton, FL, 2011).
[28]*Springer Handbook of Acoustics*, 2nd ed., edited by F. Dunn, Thomas Rossing, W. M. Hartmann, D. M. Campbell, and N. H. Fletcher (Springer-Verlag, Berlin Heidelberg, 2014).
[29]Aneesur Rahman and Frank H. Stillinger, "Propagation of sound in water. A molecular-dynamics study," Phys. Rev. A **10**(1), 368–378 (1974).
[30]J. Teixeira, M. C. Bellissent-Funel, S. H. Chen, and B. Dorner, "Observation of new short-wavelength collective excitations in heavy water by coherent inelastic neutron scattering," Phys. Rev. Lett. **54**(25), 2681–2683 (1985).
[31]Giancarlo Ruocco and Francesco Sette, "The high-frequency dynamics of liquid water," J. Phys.: Condens. Matter **11**(24), R259–R293 (1999).
[32]S. C. Santucci, D. Fioretto, L. Comez, A. Gessini, and C. Masciovecchio, "Is there any fast sound in water?," Phys. Rev. Lett. **97**(22), 225701 (2006).
[33]R. Zaleski, "Principles of positron porosimetry," Nukleonika **60**(4), 795–800 (2015).
[34]David W. Gidley, Hua-Gen Peng, and Richard S. Vallery, "Positron annihilation as a method to characterize porous materials," Ann. Rev. Mat. Res. **36**(1), 49–79 (2006).
[35]David J. Griffiths, *Introduction to Elementary Particles*, 2nd ed. (Wiley-VCH, Weinheim, Germany, 2008).
[36]Sultana N. Nahar and Bobby Antony, "Positron scattering from atoms and molecules," Atoms **8**(2), 29 (2020).
[37]David B. Cassidy and A. P. Mills, "The production of molecular positronium," Nature **449**(7159), 195–197 (2007).
[38]C. V. Shank, R. Yen, and Ch Hirlimann, "Time-resolved reflectivity measurements of femtosecond-optical-pulse-induced phase transitions in silicon," Phys. Rev. Lett. **50**(6), 454–457 (1983).
[39]A. Rousse, C. Rischel, S. Fourmaux, I. Uschmann, S. Sebban, G. Grillon, Ph. Balcou, E. Förster, J. P. Geindre, P. Audebert, J. C. Gauthier, and D. Hulin, "Non-thermal melting in semiconductors measured at femtosecond resolution," Nature **410**(6824), 65–68 (2001).
[40]Nikita Medvedev, Zheng Li, and Beata Ziaja, "Thermal and nonthermal melting of silicon under femtosecond x-ray irradiation," Phys. Rev. B **91**(5), 054113 (2015).
[41]R. L. Workman *et al*., "Review of particle physics," Prog. Theor. Exp. Phys. **2022**, 083C01.
[42]Steven Weinberg, *The Discovery of Subatomic Particles*, 2nd ed. (Cambridge U.P., Cambridge, UK, 2003).
[43]J. Marteau, D. Gibert, N. Lesparre, F. Nicollin, P. Noli, and F. Giacoppo, "Muons tomography applied to geosciences and volcanology," Nucl. Instrum. Methods Phys. Res., Sect. A **695**, 23–28 (2012).
[44]M. Morjean, D. Jacquet, J. L. Charvet, A. L'Hoir, M. Laget, M. Parlog, A. Chbihi, M. Chevallier, C. Cohen, D. Dauvergne, R. Dayras, A. Drouart, C. Escano-Rodriguez, J. D. Frankland, R. Kirsch, P. Lautesse, L. Nalpas, C. Ray, C. Schmitt, C. Stodel, L. Tassan-Got, E. Testa, and C. Volant, "Fission time measurements: A new probe into superheavy element stability," Phys. Rev. Lett. **101**(7), 072701 (2008).
[45]Paul Busch, "The time-energy uncertainty relation," in *Time in Quantum Mechanics* (Springer-Verlag, Berlin Heidelberg, Germany, 2008), pp. 73–105.
[46]M. Duer, T. Aumann, R. Gernhäuser, V. Panin, S. Paschalis, D. M. Rossi, N. L. Achouri, D. Ahn, H. Baba, C. A. Bertulani, M. Böhmer, K. Boretzky, C. Caesar, N. Chiga, A. Corsi, D. Cortina-Gil, C. A. Douma, F. Dufter, Z. Elekes, J. Feng, B. Fernández-Domínguez, U. Forsberg, N. Fukuda, I. Gasparic, Z. Ge, J. M. Gheller, J. Gibelin, A. Gillibert, K. I. Hahn, Z. Halász, M. N. Harakeh, A. Hirayama, M. Holl, N. Inabe, T. Isobe, J. Kahlbow, N. Kalantar-Nayestanaki, D. Kim, S. Kim, T. Kobayashi, Y. Kondo, D. Körper, P. Koseoglou, Y. Kubota, I. Kuti, P. J. Li, C. Lehr, S. Lindberg, Y. Liu, F. M. Marqués, S. Masuoka, M. Matsumoto, J. Mayer, K. Miki, B. Monteagudo, T. Nakamura, T. Nilsson, A. Obertelli, N. A. Orr, H. Otsu, S. Y. Park, M. Parlog, P. M. Potlog, S. Reichert, A. Revel, A. T. Saito, M. Sasano, H. Scheit, F. Schindler, S. Shimoura, H. Simon, L. Stuhl, H. Suzuki, D. Symochko, H. Takeda, J. Tanaka, Y. Togano, T. Tomai, H. T. Törnqvist, J. Tscheuschner, T. Uesaka, V. Wagner, H. Yamada, B. Yang, L. Yang, Z. H. Yang, M. Yasuda, K. Yoneda, L. Zanetti, J. Zenihiro, and M. V. Zhukov, "Observation of a correlated free four-neutron system," Nature **606**(7915), 678–682 (2022).
[47]Elizabeth Gibney, "How many yottabytes in a quettabyte? Extreme numbers get new names," Nature (2022), <https://www.nature.com/articles/d41586-022-03747-9>.